"Zorbas" on Southeastern Sicily

Subjects: Geology
Contributor: Giovanni Scardino

Over the last few years, several authors have presented contrasting models to describe the response of boulders to extreme waves, but the absence of direct observation of movements has hindered the evaluation of these models. The recent development of online video-sharing platforms in coastal settings has provided the opportunity to monitor the evolution of rocky coastlines during storm events. In September 2018, a surveillance camera of the Marine Protected Area of Plemmirio recorded the movement of several boulders along the coast of Maddalena Peninsula (Siracusa, Southeastern Sicily) during the landfall of the Mediterranean tropical-like cyclone (Medicane) Zorbas. Unmanned autonomous vehicle (UAV) photogrammetric and terrestrial laser scanner (TLS) surveys were performed to reconstruct immersive virtual scenarios to geometrically analyze the boulder displacements recorded in the video. Analyses highlighted that the displacements occurred when the boulders were submerged as a result of the impact of multiple small waves rather than due to a single large wave. Comparison between flow velocities obtained by videos and calculated through relationships showed a strong overestimation of the models, suggesting that values of flow density and lift coefficient used in literature are underestimated.

Keywords: coastal boulders ; Zorbas ; Hydrodynamic

1. Introduction

Mediterranean hurricanes, also called Mediterranean Tropical Like Cyclones (TLCs) or medicanes, are warm-core cyclones that develop over the Mediterranean Sea [1][2][3][4] with characteristics similar to tropical cyclones. Such storms are constituted by rotating cloud systems characterized by gale force winds, severe precipitation, and a low pressure center, accompanied by a spiral pattern of thunderstorms [5][6][7][8][9]. Two specific areas appear to be the favored locations for medicane genesis: the western Mediterranean [10][11] and the central Mediterranean–Ionian Sea [12][13]. During the last decades, the impacts of medicanes along the coasts of Mediterranean basin have strongly influenced the human settlements, causing a lot of damage and casualties [14][15]. Moreover, several authors predict that, in the next future, climate changes could modify medicanes, decreasing the frequency of their occurrence but increasing the strength of their impacts [4][16][17]. In the last 10 years, two dierent medicanes made landfall along the coast of Southeastern Sicily; the first one occurred in 2014 and was called Qendresa, and the second occurred in 2018 and was called Zorbas. In September 2018, Medicane Zorbas impacted the Ionian coasts of Southeastern Sicily and was registered along the coasts of Apulia, Basilicata, and Calabria with minor energy [18]. Evidence of this storm event was observed along the rocky coast of the Maddalena Peninsula (Siracusa, southeastern Sicily; Figure 1), where a surveillance camera of the Marine Protected Area of Plemmirio recorded several boulder displacements that occurred inside an ancient Greek quarry. This coastal sector is characterized by the presence of important boulder fields, interpreted as evidence of the impact of severe storms and tsunami events in the past [19][20]. Since 2009, the ancient quarry has been intensely monitored, using several survey techniques, to identify and analyze boulder displacements with the main purpose to verify if storm waves could be responsible for the movement of boulders which have been attributed to tsunami events [21].

A determination if storm or tsunami waves were responsible for the boulder displacements on coastal area has been the object of considerable debate. Several studies agree that severe storms are generally able to displace most of the small boulders found along coastlines all over the world [11][22][23][24][25][26][27]. Some authors proposed that, although boulder displacements occur both during storm and tsunami events, the main cause for movements of the biggest boulders are probably tsunami [15][27]. In contrast, other studies ascribe storms the capability to detach and transport the boulders [28]. A new debate has been recently opened on the number of tsunami events reconstructed for the Mediterranean Sea. Marriner et al. [29] consider this number strongly overestimated, contesting the attribution to tsunami of most of the field evidences described in the literature, and suggesting that cyclical periods of increased storminess, driven by late Holocene climate changes, would be responsible for them.

Vött et al. [30] replied to this theory disputing the tsunami DB and the statistical analyses used by Marriner et al. [31], confirming the reliability of the literature in the definition of tsunami events occurred in the Mediterranean Sea.

The Mediterranean basin, due to the lack extreme events such as cyclones, has been considered an excellent area for studies aimed to describe tsunami events [32]. In the absence of observatories, the analytical approach for the study boulder displacements has been the application of different hydrodynamic models (e.g., references [33][34][35][36][37]) to estimate the main features of the wave responsible for the dislocation (Typology, Wave Height, Wave flow velocity). To apply these models it is fundamental to acquire high-resolution data of the boulders (size, volume and mass), but it is also very important to reconstruct (i) the scenario in which the movement occurred (joint bounded or subaerial/submerged); (ii) the typology of movement (sliding, rolling/overturning, saltation/lifting); and (iii) the entity of displacement. These parameters are often very complicated to deduct by field evidence [38][39]. Up to the present, all the studies started from the assumption that the different position of a boulder, after and before an extreme marine event, represents the effect of a single wave impact [40][41][42]. For these reasons, until now, it has been very dicult to test the reliability of the hydrodynamic models in the description of the natural processes.

The aim of this work is to overcome this problem through the analyses of video recorded along the Maddalena Peninsula. Given that video witness has never been used before to analyze boulder displacements, we defined a methodology to reconstruct immersive scenarios, useful for georeferencing the images recorded in the video and to accurately measure, from them, several important parameters such as the wave heights at time of impacts and the wave flows at time of displacements. This kind of approach let us accurately test hydrodynamic equations, showing a significant overestimation of them, probably due to an underestimation of important parameter, such as seawater flow density and lift coefficient [43][44][45].

Furthermore, the work provides evidence about the dynamics of boulder movements, suggesting that single wave impacts are unlikely to be responsible for displacements, which normally occur as a result of multiple waves impact, generating a turbulent flow able to nullify frictions. In addition, our work shows that some boulders, previously interpreted as deposited by a tsunami event, have never been displaced in 10 years of monitoring, and so accord with the hypothesis that only tsunamis could be responsible for the deposition of boulders with particular features as dimension and shape.

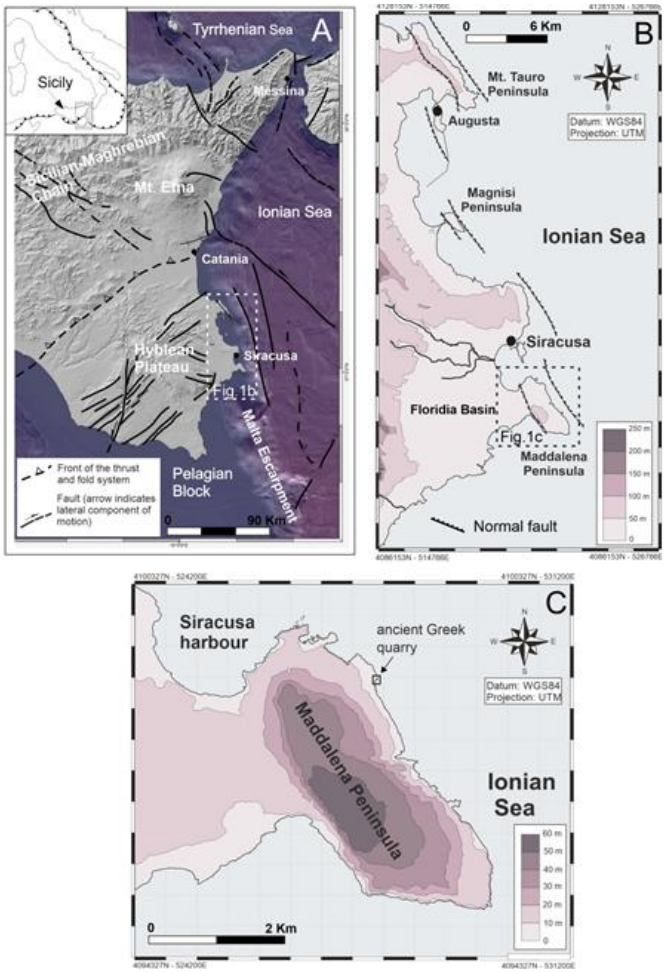

Figure 1. Geological settings of Southeastern Sicily. (**A**) Tectonic sketch map of the Sicilian Collision Zone in eastern Sicily (from Cultrera et al. [46], modified). (**B**) Position of the Maddalena Peninsula area along the Ionian coast of southeastern Sicily. (**C**) Morphological map of the Maddalena Peninsula showing the location of the study area (box).

2. Geological Settings

Southeastern Sicily (Figure 1A) is part of the emerged portion of the Pelagian Block, the foreland domain of the Neogene-Quaternary Sicilian Collision Zone. It is mostly formed by the Hyblean Plateau that along the Ionian coastline is dissected by a system of Quaternary normal faults bounding NNW–SSE oriented horst and graben structures [47]. The Maddalena Peninsula, constituted by a Neogene-Quaternary calcareous succession, is one of the horst structures located along the Ionian coast of southeastern Sicily (Figure 1B). The whole area lies at the footwall of a large normal fault system that, since the Middle Pleistocene, has reactivated the Malta Escarpment [48], a large Mesozoic boundary separating the Pelagian Block from the Ionian oceanic domain to the East [49][50]. Southeastern Sicily is one of the most seismically active areas of the central Mediterranean. It is characterized by a high level of crustal seismicity producing earthquakes with intensities of up to XI–XII Mercalli-Cancani-Sieberg (MCS) and M ~7, such as the 1169, 1693, and 1908 events [51][52][53] and related tsunami [21][54][24][55][56]. Being located along a collisional belt, at the footwall of a normal fault system, the analyzed coastal area has experienced vertical deformation that, combined with sea-level changes, has been recorded by several orders of Middle-Upper Quaternary marine terraces and palaeo-shorelines [57][58][59][60]. However, since the Late Pleistocene the Maddalena Peninsula (Figure 1C) was tectonically stable, as inferred from the elevation of the MIS 5.5 terraces [61] but lightly uplifting in the Holocene [26][62][63][64]. According to Anzidei et al. [65], during the last few decades, Global Positioning System (GPS) data and Glacial Isostatic Adjustment (GIA) models indicated current weak subsidence at rates close to 1 mm/yr. This is relevant considering that the area is undergoing heavy coastal retreat and so is exposed to severe storms associated with high-waves, also as a consequence of the global sea-level rise [66][67][68][69]. The Ionian coast of Southeastern Sicily, between the towns of Augusta and Siracusa, is characterized by the occurrence of anomalous calcareous and calcarenitic boulders. Scicchitano et al. [54] performed direct observations on these boulders (distance from the coastline, size and weight), together with statistical analysis of the storm regime of the area and hydrodynamic estimations, to verify if tsunami or storm waves were responsible for their detachment and transport. Radiocarbon age determinations of marine organisms encrusting the blocks, compared to historical catalogues, suggested that, in the last 1000 years, the largest earthquakes with local sources (e.g., the 1169, 1693, and 1908 events) could have triggered tsunami waves that displaced the largest boulders occurring in the area. Other evidence of these tsunami events were found along the coasts of Southeastern Sicily, inside several lagoons [70][71][72] and in coastal deposits [73].

Along Maddalena Peninsula, boulder deposits usually occur on large surfaces gently sloping towards the sea, bordered by high cliffs up to 5 m, formed by Pleistocene depositional terraces or rock platforms dissecting Neogene sub-horizontal, well-stratified, and fractured limestones. The surveillance camera detected boulder displacements inside an ancient Greek quarry located in the northern sector of the Maddalena Peninsula, whose floor has been partially submerged by Holocene sea level rise (up to 40 cm [74]). Boulders located inside the quarry were surveyed with terrestrial laser scanner (TLS) techniques in order to estimate, through the use of a specific hydrodynamic equation [41], the inland penetration limit of the tsunami responsible for the deposition of the block. The two biggest boulders surveyed inside the quarry were represented by a boulder of about 13 ton in weight, previously attributed to a tsunami impact [21], and a boulder of about 41 ton displaced in January 2009 by a storm. Hydrodynamic analyses performed by several authors reveal that coasts of Southeastern Sicily can be affected by severe storm which generate waves able to detach large blocks from the coastal edge and transport them inland [21][54][75][76][77][78].

For the Ionian coast of Sicily, significant spectral wave height (Hm0) and peak period (Tp), recorded during the last 18 years by the Catania buoy (RON—Rete Ondametrica Nazionale; www.idromare.com), are available (Figure 2A). Wave data recorded by the Catania buoy indicated that the most severe storm, which occurred on 2 February 1996, was characterized by significant spectral wave height (Hm0) of about 6.2 m and peak period Tp = 11.3 s. According to Inglesi et al. [79], the return value Hm0 (50) corresponding to a return period of 50 years in the Catania sector do not exceed 6.24 m. A monitoring operated at the quarry located on Maddalena Peninsula indicated that the main boulder displacements have occurred as result of three distinct storms that occurred in 2009, 2014, and 2018. The events of 2014 and 2018 were two medicanes, called Qendresa and Zorbas, respectively. Qendresa formed on 5 November and rapidly intensified two days later, reaching peak intensity on 7 November. It directly hit Malta in the afternoon and then crossed the Eastern coast of Sicily on 8 November. Later, the cyclone weakened significantly and dissipated over Crete on 11 November. Measurements taken by the ondametric buoy of Crotone and Catania (RON—Rete Ondametrica Nazionale; www.idromare.com; Figure 2B), during the passage of Qendresa, show values of significant spectral wave height Hm0 of about 4 m. Medicane Zorbas emerged into the Aegean Sea, moved westward to reach the center of Ionian sea, then inverted its track, moving over northwestern Turkey. Although Zorbas did not affect southeastern Sicily directly, as in the case of Medicane Qendresa, its impact induced similar effects, as recorded by satellite data in off-shore (significant wave

height Hs of about 4.1 m) (source AVISO satellite altimetry, credits CLS/CNES). Another relevant effect induced by Zorbas was a storm surge, up to 1m above, detected by the tide gauge sited inside Catania harbor (Figure 2C) and also observed in the video recorded in the Maddalena Peninsula.

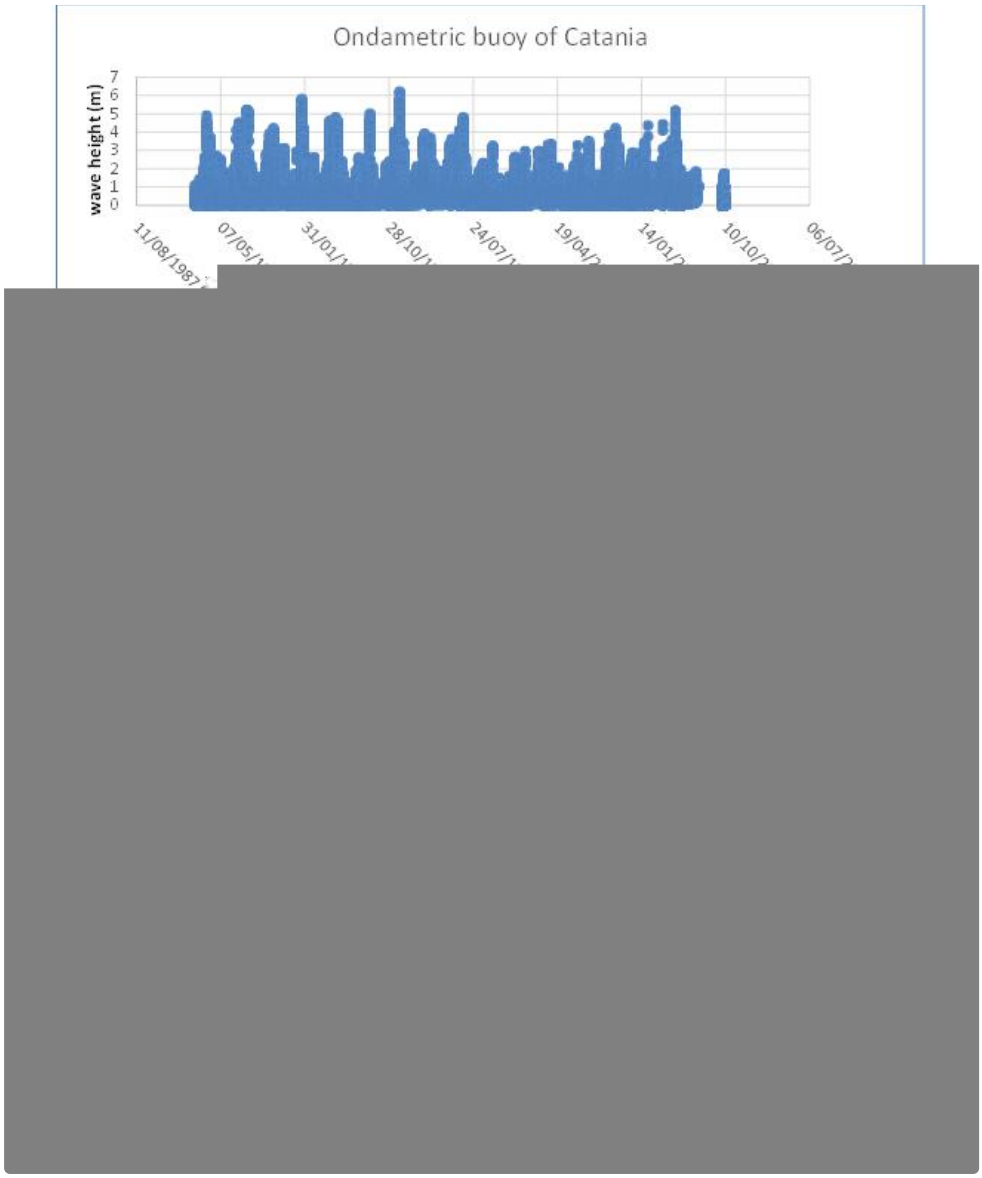

Figure 2. Meteo-marine features recorded in Southeastern Sicily. (**A**) Data of significant spectral wave heights Hm0 recorded by ondametric buoy of Catania (1986–2006). (**B**) Wave height Hm0 recorded by Catania buoy (RON) during Medicane Qendresa. (**C**) Sea level recorded by tide gauge of Capo Passero (ISPRA) during Medicane Zorbas.

3. Material and Methods

In 2003, the technicians of the Marine Protected Area of Plemmirio installed 10 surveillance stations along the coasts of Maddalena Peninsula with the aim to detect illegal fishing operations and to monitoring sea conditions. One of these stations was positioned in proximity of the ancient Greek quarry sited in the northern sector of the Maddalena Peninsula (Figure 3A). The stations are mounted 9 m high on a pole (Figure 3B) and equipped with a HDTV camera (Figure 3C) with 30x optical zoom framing the coastal area (lens 4.3–129 mm; F1.6–4.7; horizontal field of view: 65.6°–2.0°; vertical field of view: 39.0°–1.2°). During 28 September 2019, the camera recorded about 4 h of video during the Medicane Zorbas. Analyses of this video identified 28 boulder movements inside the quarry. Some of these boulders were already present, and they had been attributed both to tsunami and storm events [21]. The others were detached from the submerged area and transported inland during the Medicane Zorbas. In order to proceed with the analysis of the videos extracted from the Control Center Data Base (resolution 1920 × 1080, frame rate of 25 fps, 50 Hz), it has been necessary to reconstruct a detailed and accurate immersive virtual scenario of the quarry and of the boulders, pre and post the impact of Medicane Zorbas. In 2009, the northern sector of the Maddalena Peninsula was surveyed using Terrestrial Laser Scanner (TLS) techniques in order to reconstruct the morpho-topographic features of the quarry and of the boulders inside it. The survey was performed by scanning the area from four different points, located on the top of the quarry and from two other points sited inside it. The complete TLS dataset was treated and analyzed by using HDS Cyclone software in order to remove any outliers such as vegetation or anthropogenic features. Then, a dense cloud of points was generated permitting the

reconstruction of a 3D model of the quarry and of the boulders present in it. Moreover, since the acquisition of TLS data, we started to monitor the boulder positions inside the quarry by surveying after every storm event, through RTK-GPS techniques, benchmarks located on boulders reconstructed with TLS. In January 2015, a few months after the Medicane Qendresa (8 September 2014), we performed UAV photogrammetric surveys of the quarry to detect the position of the boulders displaced during the Medicane. The results convinced us to replace TLS with UAV photogrammetry techniques (cheaper than TLS and with similar resolution and accuracy) to monitor boulder movements occurring inside the quarry. With this aim, we performed surveys in 2016–2018.A pre-impact virtual immersive scenario has been modelled combining cloud points reconstructed with TLS in 2009 with the cloud points detected with the UAV photogrammetric surveys performed on 2017. This scenario was used to detect in the video morphological features, such as the edges of the quarry, useful as benchmarks to geometrically analyze, through specific software, the images recorded in the video showing boulder movements. To reconstruct the post-impact virtual immersive scenario we performed, three days after the impact of the Medicane Zorbas, an UAV photogrammetric survey (Figure 3D) of the quarry area together with a proximity photogrammetric survey of the new boulders displaced on the coast. Geographic Information System (GIS) analyses of the products of previous and recent surveys let us identify most of the boulders appearing in the recorded video (the others have probably been fragmented into smaller blocks). The video has been analyzed by Tracker (https://physlets.org/tracker/), a video analysis and modelling software built on the Open Source Physics (OSP, Doug Brown, Cabrillo College, California, U.S.) Java framework. Distance between specific features clearly visible in the video, as for example quarry edges, holes, and fractures, were inserted as a spatial reference in Tracker. Once defined, the spatial reference, tagging in each frame of the video objects in motion (boulders, waves, and flows), the software is able to calculate velocity and accelerations. We focused our analyses on the estimation of the flow velocity at time boulder movements occurred. From the assessment of boulder features, we have calculated, through the hydrodynamic equations of Nandasena et al. [35], the flow needed to start the movements of the blocks analyzed in the videos. Flow values estimated trough video analyses were compared with those calculated with the Nandasena et al. [35] model in order to evaluate the possible discrepancies.

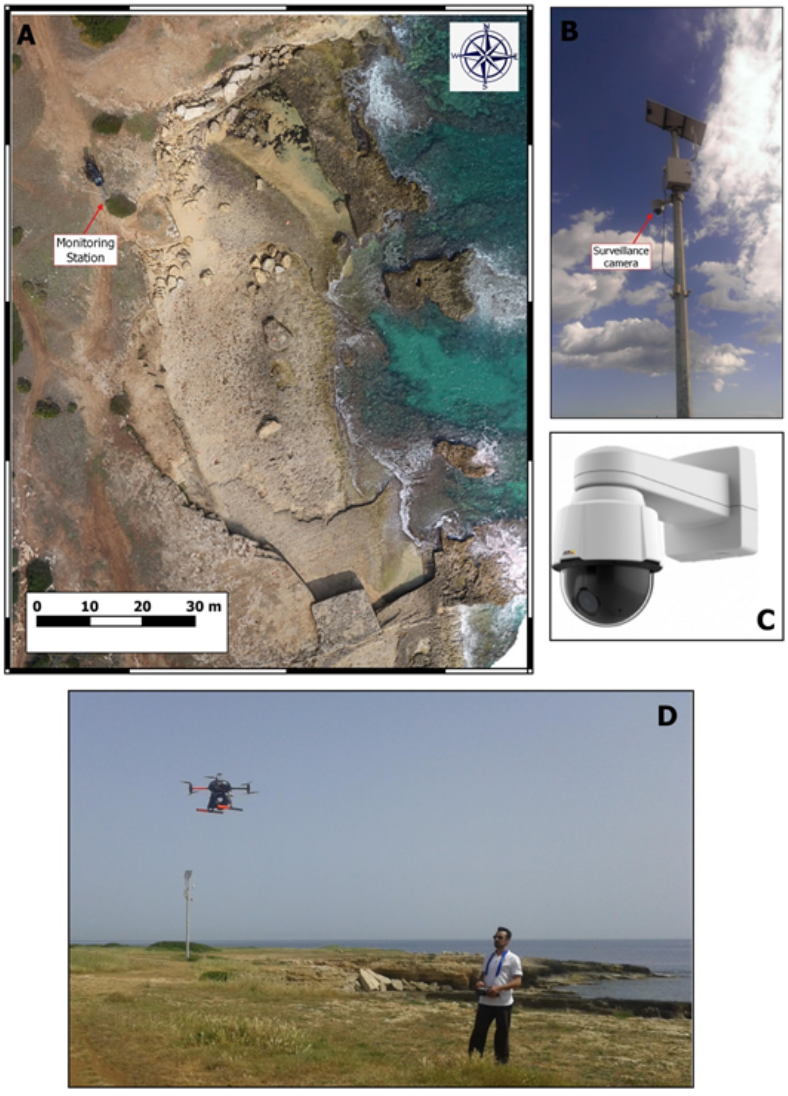

Figure 3. (**A**) Orthophoto (Resolution 1cm/pxl) of ancient Greek quarry located in the northern sector of the Maddalena Peninsula, the arrow shows the Monitoring Station. (**B**) Monitoring Station mounted on pole at 9m height. (**C**) HDTV camera. (**D**) Unmanned Autonomous Vehicle (UAV) survey operations in the studied area, the pole with Monitoring Station

is also visible.

3.1. UAV Data and GIS Analyses

The use of Unmanned Autonomous Vehicles (UAV), better known as drones, in various fields of geoscience has increased during the last five years. In coastal geomorphology studies, UAV photogrammetry techniques have been applied for flood estimation [80][22] and for boulder field monitoring [75][23]. Since 2015, the area of study has been seasonally monitored with UAV photogrammetry surveys in order to detect boulder movements inside the Greek quarry sited in Maddalena Peninsula. Considering the large number of boulders displaced during the impact of the storm generated by the Medicane Zorbas, we performed an UAV survey three days after the storm. The survey was performed with a Multicopter NT4 Airvision (Studio Geologi Associati T.S.T., Catania, Italy) (Figure 3), equipped with an High Definition camera (resolution 24Mpx, lens 16 mm, f3, 5–5, 6), that flew at 30m of altitude, during four distinct flights, with a speed of 1.5 m/s.

In order to obtain an accurate georeferencing of the UAV data, we used the ground control point (GCP) net installed in 2015 and composed of 40 benchmarks regularly spaced along the quarry area (Figure 4A). Benchmarks positions were surveyed with real-time kinematic (RTK) GPS performing 1 h of acquisition for each point of the net. Colored markers, visible from 30 m of altitude, were placed on the benchmarks (Figure 4B) before realizing the flights. A total of 152 pictures were collected and processed using Agisoft Photoscan Professional software version 1.4.0 (St. Petersburg, Russia) to obtain a high-resolution digital elevation model (DEM, 2 cm grid cell; Figure 5A) and orthophotographs (1 cm/pxl; Figure 5B).

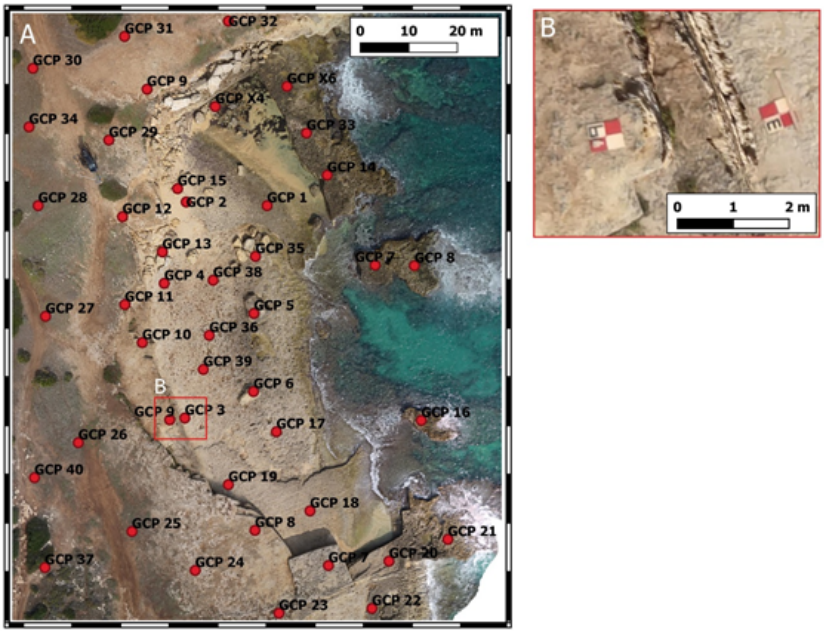

Figure 4. (**A**) Ground control point (GCP) net installed in 2015 and composed of 40 benchmarks regularly spaced along the quarry area. (**B**) Detail of the colored markers positioned on the ground.

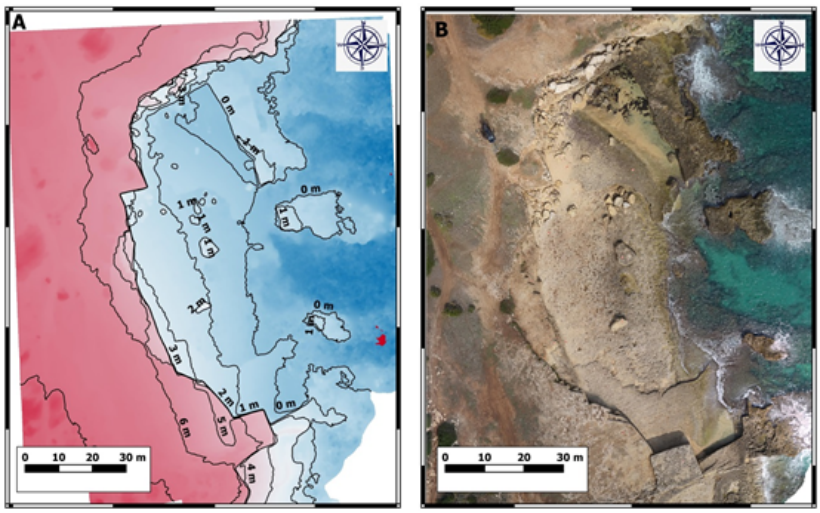

Figure 5. (**A**) High-resolution digital elevation model (2 cm grid cell). (B) Orthophotographs (resolution 1 cm/pxl) reconstructed by UAV photogrammetric survey.

These two products were integrated into the general Geo Data Base developed in 2009 and composed by (i) orthophotos and DEM obtained by TLS (2009) and UAV surveys (2015–2018); (ii) orthophotos provided by Regione Sicilia (2007, 2008, 2013); (iii) RTK-GPS data of boulder positions and displacements (2009–2018); and (iv) a 3D model of all boulders dislocated inside the quarry since 2009. Morpho-topographic surveys were performed every year and interpreted in the GIS environment (QGIS) through the digitalization of all the main morphological features such as boulders, fractures, detached part of coastline, score marks and sediment accumulations. These features have been compared with those extracted from the orthophotographs and DEM obtained in the previous year to identify boulder movements or other changes in coastal landscape. As it is possible to observe in Figure 6, several boulders were displaced in the studied area for effects of the impact of Medicane Zorbas; some of these were already in the area and moved from their original position, while others were detached from the infralittoral zone and deposited on the coastline.

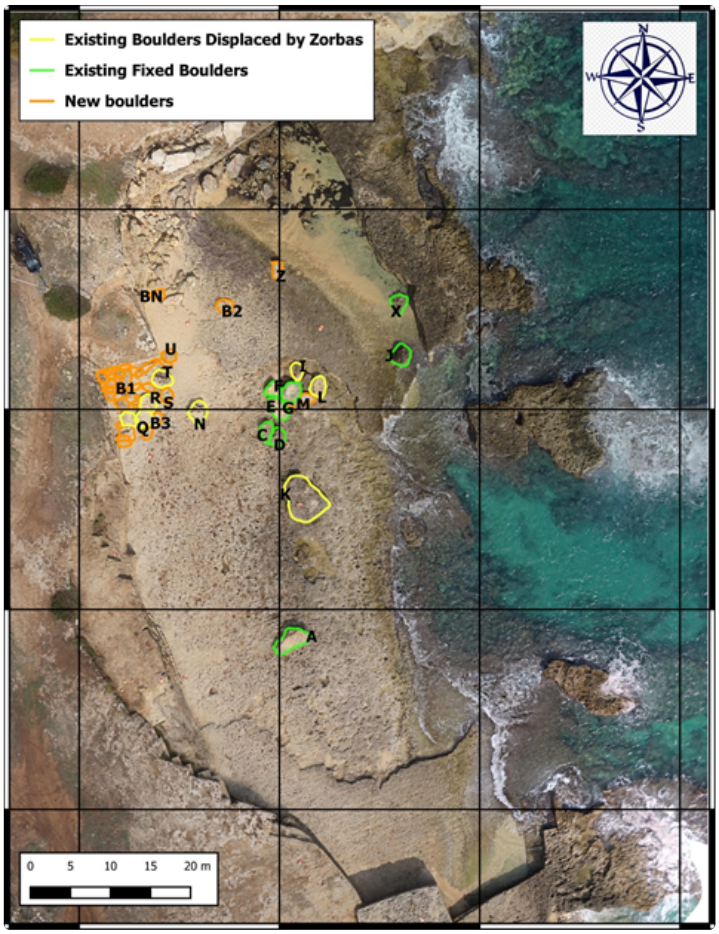

Figure 6. Boulders edited in Quantum Geographic Information System (QGIS) from the Orthophoto reconstructed after the impact of Medicane Zorbas; the boulders already present on the coastline and displaced by Zorbas are marked in yellow, the boulders detached from the coastline and dispersed on the shore-platform by Zorbas are marked in orange, and the boulders not displaced by Zorbas are marked in green.

3.2. Boulders Survey

Once identified in the most recent orthophoto, the new boulders dispersed on the coastline by the impact of Medicane Zorbas have been surveyed with photogrammetry techniques to accurately calculate volume, dimension, and organic encrustations. Pictures were collected with an High Definition camera (resolution 24Mpx, lens 16mm, f3,5-5,6). Around each boulder, 38 benchmarks were positioned on the boulders and surveyed with a total station for georeferencing the reconstructions of the blocks. Pictures and Benchmarks were processed in Agisoft Photoscan Professional software version 1.4.0 (Figure 7A) to obtain high-resolution 3D surface of the boulders and then post processed in Rhino 6 (Rhino Software 6, Mc Neel Europe, Barcellona, Spain) to close holes and missed surface and generate the final 3d model (Figure 7B). Determination of bulk density was carried out on rock samples collected from the surveyed boulders. The volume of rock samples was determined through the Instantaneous Water Immersion Method [25]. The mass of each boulder was estimated as the product of boulder's density and volume. Density was assigned to each boulder on the basis of results of bulk density measurements as well as considering its thickness and lithology (Table 1).

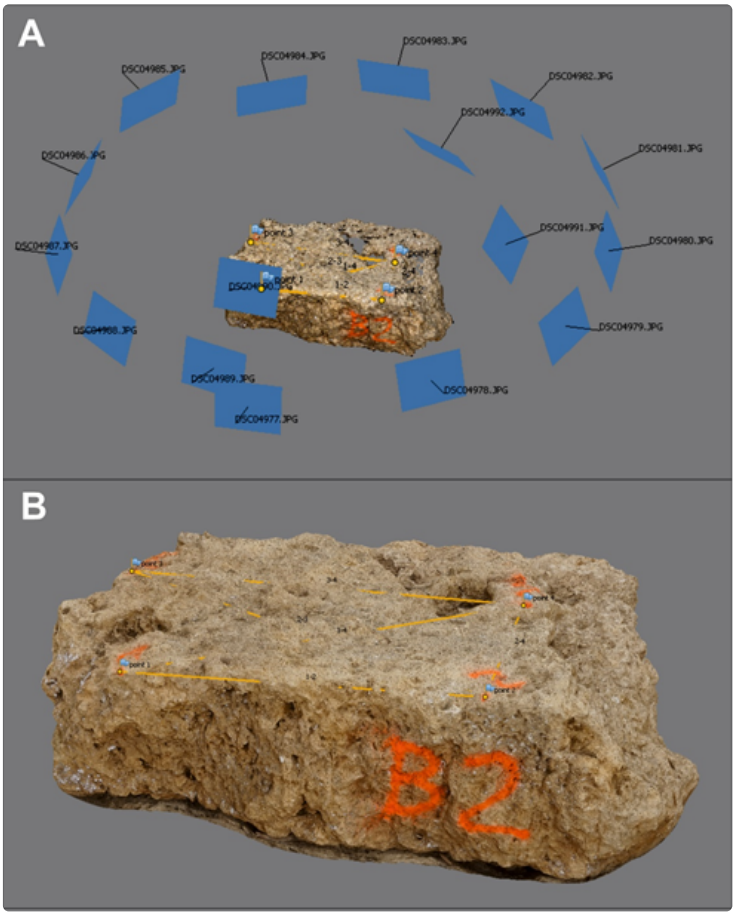

Figure 7. (**A**) Pictures (blue rectangles) and benchmarks (light blue flags) processed in Agisoft Photoscan Professional software version 1.4.0. (**B**) Three-dimensional model of boulder B2 reconstructed with Rhino 6.

Table 1. Boulder features detected through photogrammetry surveys and laboratory analysis.

ID	Volume (m^3)	Density (kg/m^3)	Masses (kg)	a-Axis (m)	b-Axis (m)	c-Axis (m)	a-Axis Direction
BN	0.367	2080	763.36	1.8	0.95	0.3	N110E
B2	0.705	2080	1466.4	1.5	1.17	0.42	N120E
B3	0.828	2040	1689.12	1.9	0.96	0.45	N210E
B4	0.569	2070	1177.83	1.57	0.97	0.4	N190E
D	2.283	2040	4657.32	2.4	1.95	1	
F	1.461	2040	2980.44	2.1	1.9	0.6	N354E
H	3.377	2040	6889.08	2.6	2.4	0.9	
L	0.89	2040	1815.6	2.5	1.6	0.5	N338E
N	4.031	2040	8223.24	3.2	2.2	1.15	N281E
J	3.367	2040	6868.68	2.2	2.1	1.25	
X	1.61	2040	3284.4	2.2	1.95	0.7	

K	18.782	2200	41320.4	5.8	5.18	1.3	N159E

3.3. Video Editing

More than 7 h of consecutive video recorded on 28 September 2019 were analyzed, detecting 28 distinct boulder movements occurred in the Greek quarry (Table 2). In particular, we focused on five boulders, for which a reliable identification in field and in the orthophoto was possible. Boulders B2, B3, B4, and BN were not present on the coastline before the impact of Zorbas. Boulder K is a very large block, about 41 ton in weight, first displaced by a storm in 2009 and moved again by the two medicanes (2014 and 2018). Videos highlighted the wave impacts on the Greek quarry and showed the boulder movement that occurred in subaerial/submerged scenario. In the video frames, the moment of boulder movements is visible, which occurred with a clear wet surface caused by a continuous wave flow impacting. At the moment of boulder movement, wave flow assumed a turbulent motion with main directions from SE and E, with subsequent backwash flow detected in different directions.

Table 2. Results of video analyses of boulder displacements detected in the Maddalena Peninsula.

No.	Video Time Frame	Boulder	Movement Dynamics	Found in Field	Flow u (m/s)
1	14:21:37.221–14:21:50.945	B1	Sliding	NO	
2	14:29:32.769–14:29:44.885	B1	Sliding/overturning	NO	2.012
3	14:31:08.964–14:31:13.264	B1	Overturning	NO	1.71
4	14:33:11.857–14:33:16.157	B1	Saltation	NO	1.29
5	14:35:32.948–14:35:36.648	B1_F	Overturning	NO	1.588
6	14:41:13.447–14:41:15.147	B1	Overturning	NO	2.113
7	15:01:18.471	B1	Saltation	NO	
8	15:02:17.148–15:02:18.948	B2	Overturning	NO	2.101
9	15:14:57.718-15:15:04.118	B2	Overturning	NO	1.687
10	15:51:53.464	B1_F	Saltation	NO	1.783
11	15:52:46.083	B2	Saltation	YES	2.101
12	15:57:57.546–15:58:02.145	B3	Sliding	YES	
13	15:59:05.542–15:59:07.342	B3	Sliding	YES	2.58
14	15:59:16.666	B3	Sliding	YES	
15	16:05:17.440–16:05:24.040	B3	Overturning	YES	1.663
16	16:08:04.024–16:08:34.941	B3	Overturning/Sliding	YES	2.331

17	16:16:17.351–16:16:23.504	B3	Overturning	YES	1.305
18	16:16:57.984–16:17:05.536	BN	Overturning	YES	1.981
19	16:18:08.880–16:18:13.080	B3	Overturning/Sliding	YES	
20	16:26:28.971	B3	Overturning/Sliding	YES	
21	16:28:04.317–16:28:14.854	BT	Overturning	NO	1.345
22	16:28:30.688–16:28:44.506	BT	Overturning	NO	2.269
23	16:31:27.882	B3	Overturning	YES	
24	16:31:30	K	Sliding	YES	4
25	17:41:35.526	B4	Saltation	YES	
26	17:42:45.483–17:42:52.613	B4	Saltation	YES	
27	17:49:26.616–17:49:36.252	B4	Overturning	YES	
28	18:16:30	B4	Sliding	YES	2.525

Video analysis has been performed by means of Tracker software (Doug Brown, Cabrillo College, California, U.S.) using as metric reference the measures of the quarry borders detected by TLS data and some other specific features recognizable on the bedrock of the quarry (Figure 8). Metric references were selected very close to the boulders displaced in the video in order to avoid issues related to perspective distortion that could induce significant errors in the measurements of flow velocity. Videos were acquired with a frequency of 25 fps; detecting a fixed point on the boulders in each frame, it was possible to assess the wave flow velocity, wave period, wave height, velocity, and acceleration of boulders when they start to move. For boulders B2, B3, B4, and BN, we selected the movement showing highest values of flow velocity as reported in Table 3. Boulder K moved just one time, but, unfortunately, the presence of strong turbulence at that time did not permit us to evaluate the flow for each frame of the video. In this case, velocity was calculated considering distance and time between two clearly visible frames.

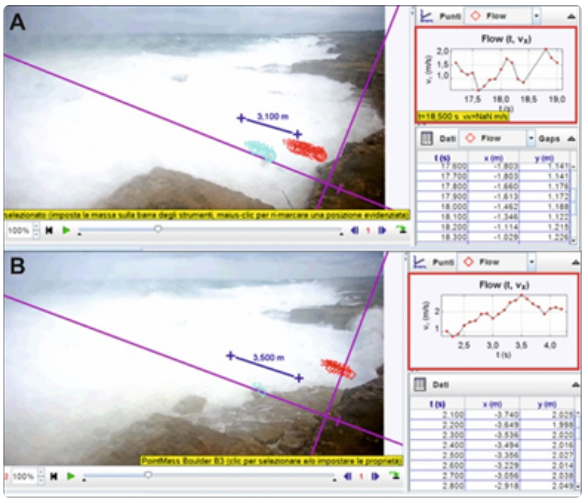

Figure 8. Editing analysis of video frames during boulder movements through Tracker software. (**A**) Rolling of boulder B2 at hour 15:02:00 UTC; (**B**) movement of boulder B3 at hour 16:16:00 UTC. In the red box diagrams are showed the flow velocity estimations marked for each frame of the video.

3.4. Hydrodynamic Models

In the last few years, several hydrodynamic models have been proposed by different authors to describe boulders displacement in coastal areas as result of the propagation of an extreme wave [28][81][43][35][82]. Nandasena et al. [35], in particular, elaborated a model to calculate the flow velocity needed to start the movement of a boulder for various dynamics of movement (sliding, rolling/overturning, saltation/lifting) and different pre-settings conditions of the boulder (the joint-bounded-JB, subaerial/submerged-SB). At the present, the main limit for applying Nandasena et al. [35] to field evidence has been that the dynamics of the movements were not certain but reconstructed comparing the final position of a boulder with the previous position.

As exposed in the videos editing, the final position of the boulders, displaced during the Medicane Zorbas, is never related to a single wave impact, but it is the result of several different movements that occurred in different directions and with different amplitudes. In this case, we overcome this problem because, through the recorded video, it was possible to extract, for each movement, certain information about the original position and pre-setting condition of the boulder and the dynamics of the movement. Moreover, from video editing, we obtained values of flow velocity at the time of movement of the boulders that could be directly compared with values estimated by Nandasena et al. [35] model. This model has been applied to the five considered boulders in relation to five specific movements recorded in the video (Table 3), in subaerial/submerged scenario:

sliding

$$u^2 = 2(\rho_s \,/\, \rho_w - 1)gc(\mu_s cos\theta + sin\theta)/(C_d(c \,/\, b) + \mu_s C_l)$$

rolling/overturning

$$\mathbf{u^2 = \frac{2\,(\rho_s/\rho_w - 1)\,gc\,(\cos\theta + (c/b)\sin\theta)}{C_d\,(c^2/b^2) + C_l}}$$

saltation/lifting

$$\mathbf{u^2 = \frac{2\,(\rho_s/\rho_w - 1)\,gc\,(\cos\theta)}{C_l}}$$

in joint-bounded scenario

saltation/lifting

$$\mathbf{u^2 = \frac{2\,(\rho_s/\rho_w - 1)\,gc\,(\cos\theta + \mu_s \sin\theta)}{C_l}}$$

where

u is the flow velocity needed to start the boulder movement;
ρ_s is the density of the boulder;
ρ_w is the density of the water (equal to 1025 kg/m^3);
g is the gravity acceleration;
μ_s is the coefficient of static friction;
θ is the angle of the bed slope at the pre-transport location in degrees;
C_d is the drag coefficient (equal to 1.5);
$a - b - c$ are the axis of the boulder, with the convention a > b > c;
C_l is the lift coefficient (equal to 0.178).

Although some authors attributed to the wave flow the same density value for the seawater [28,29,31,32], recent work [77] has demonstrated that flow density, resulting from a mix of seawater and sediments, should be estimated as follow:

$$\rho_m = (f_s * \rho_s) + (f_w + \rho_w) \quad (5)$$

where ρ_m is the average density of the seawater and sediment mix, f_w is the seawater fraction by volume between 0 and 1, f_s is the sediment fraction by volume between 0 and 1, ρ_w is the density of clear seawater (1.025 g/cm^3), ρ_s is the sediment density, and $f_w + f_s = 1$.

References

1. J. A. Ernst; M. Matson; A MEDITERRANEAN TROPICAL STORM?. *Weather* **1983**, *38*, 332-337, 10.1002/j.1477-8696.1983.tb04818.x.
2. Oreste Reale; Robert Atlas; Tropical Cyclone–Like Vortices in the Extratropics: Observational Evidence and Synoptic Analysis. *Weather and Forecasting* **2001**, *16*, 7-34, 10.1175/1520-0434(2001)016<0007:tclvit>2.0.co;2.
3. Jansà, A; Miniciclons a la Mediterrània. *IX Jornades Meteorol. Eduard Fontserè Assoc. Catalana Meteorol. (ACAM) Barc.* **2003**, *9*, 75–85, .
4. L. Fita; Romualdo Romero; A. Luque; K. Emanuel; Climent Ramis; Analysis of the environments of seven Mediterranean tropical-like storms using an axisymmetric, nonhydrostatic, cloud resolving model. *Natural Hazards and Earth System Sciences* **2007**, *7*, 41-56, 10.5194/nhess-7-41-2007.
5. Mario Marcello Miglietta; Sante Laviola; A. Malvaldi; D. Conte; Vincenzo Levizzani; C. Price; Analysis of tropical-like cyclones over the Mediterranean Sea through a combined modeling and satellite approach. *Geophysical Research Letters* **2013**, *40*, 2400-2405, 10.1002/grl.50432.
6. Leone Cavicchia; Hans Von Storch; Silvio Gualdi; Mediterranean Tropical-Like Cyclones in Present and Future Climate. *Journal of Climate* **2014**, *27*, 7493-7501, 10.1175/jcli-d-14-00339.1.
7. Nastos, P.T.; Karavana-Papadimou, K.; Matsangouras, I.T. Tropical-like cyclones in the Mediterranean: Impacts and composite daily means and anomalies of synoptic conditions. In Proceedings of the 14th International Conference on Environmental Science and Technology, Rhodes, Greece, 3–5 September 2015.
8. Guido Cioni; P. Malguzzi; A. Buzzi; Thermal structure and dynamical precursor of a Mediterranean tropical-like cyclone. *Quarterly Journal of the Royal Meteorological Society* **2016**, *142*, 1757-1766, 10.1002/qj.2773.
9. Agata Moscatello; Mario Marcello Miglietta; Richard Rotunno; Observational analysis of a Mediterranean 'hurricane' over south-eastern Italy. *Weather* **2008**, *63*, 306-311, 10.1002/wea.231.
10. Ioannis Pytharoulis; George Craig; Susan P Ballard; The hurricane-like Mediterranean cyclone of January 1995. *Meteorological Applications* **2000**, *7*, 261-279, 10.1017/s1350482700001511.
11. Bakkensen, L.A; Mediterranean Hurricanes and Associated Damage Estimates.. *J. Extrem. Events* **2017**, *4*, 1750008, .
12. Piero Lionello; F. Giorgi; Winter precipitation and cyclones in the Mediterranean region: future climate scenarios in a regional simulation. *Advances in Geosciences* **2007**, *12*, 153-158, 10.5194/adgeo-12-153-2007.
13. Piero Lionello; Dario Conte; Luigi Marzo; Luca Scarascia; The contrasting effect of increasing mean sea level and decreasing storminess on the maximum water level during storms along the coast of the Mediterranean Sea in the mid 21st century. *Global and Planetary Change* **2017**, *151*, 80-91, 10.1016/j.gloplacha.2016.06.012.
14. Raphael Portmann; J. J. González-Alemán; Michael Sprenger; Heini Wernli; Medicane Zorbas: Origin and impact of an uncertain potential vorticity streamer. *Weather Clim. Dyn. Discuss.* **2019**, *2019*, 1-30, 10.5194/wcd-2019-1.

15. Giovanni Scicchitano; Carmelo Monaco; Luigi Tortorici; Large boulder deposits by tsunami waves along the Ionian coast of south-eastern Sicily (Italy). *Marine Geology* **2007**, *238*, 75-91, 10.1016/j.margeo.2006.12.005.

16. Giovanni Scicchitano; C. Pignatelli; Cecilia Rita Spampinato; A. Piscitelli; M. Milella; Carmelo Monaco; G. Mastronuzzi; Terrestrial Laser Scanner techniques in the assessment of tsunami impact on the Maddalena peninsula (south-eastern Sicily, Italy). *Earth, Planets and Space* **2012**, *64*, 889-903, 10.5047/eps.2011.11.009.

17. Matteo Vacchi; Alessio Rovere; N. Zouros; M. Firpo; Assessing enigmatic boulder deposits in NE Aegean Sea: importance of historical sources as tool to support hydrodynamic equations. *Natural Hazards and Earth System Sciences* **2012**, *12*, 1109-1118, 10.5194/nhess-12-1109-2012.

18. M. Shah-Hosseini; C. Morhange; A. De; J. Wante; J. Anthony E.; F. Sabatier; G. Mastronuzzi; C. Pignatelli; A. Piscitelli; Coastal boulders in Martigues, French Mediterranean: evidence for extreme storm waves during the Little Ice Age. *Zeitschrift für Geomorphologie, Supplementary Issues* **2013**, *57*, 181–199, 10.1127/0372-8854/2013/00132.

19. Sara Biolchi; Stefano Furlani; Fabrizio Antonioli; Niccolò Baldassini; Joanna Causon Deguara; Stefano Devoto; Agata Di Stefano; J Evans; Timothy Gambin; Ritienne Gauci; et al. Boulder accumulations related to extreme wave events on the eastern coast of Malta. *Natural Hazards and Earth System Sciences* **2016**, *16*, 737-756, 10.5194/nhess-16-737-2016.

20. Sara Biolchi; Stefano Furlani; Stefano Devoto; Giovanni Scicchitano; Tvrtko Korbar; Ivica Vilibić; Jadranka Šepić; The origin and dynamics of coastal boulders in a semi-enclosed shallow basin: A northern Adriatic case study. *Marine Geology* **2019**, *411*, 62-77, 10.1016/j.margeo.2019.01.008.

21. Sara Biolchi; Cléa Denamiel; Stefano Devoto; Tvrtko Korbar; Vanja Macovaz; Giovanni Scicchitano; Ivica Vilibić; Stefano Furlani; Impact of the October 2018 Storm Vaia on Coastal Boulders in the Northern Adriatic Sea. *Water* **2019**, *11*, 2229, 10.3390/w11112229.

22. Piscitelli, A.; Milella, M.; Hippolyte, J.-C.; Shah-Hosseini, M.; Morhange, C.; Mastronuzzi, G; Shah-Hosseini, M.; Morhange, C.; Mastronuzzi, G. Numerical approach to the study of coastal boulders: The case of Martigues, Marseille, France. *Quat. Int.* **2017**, *439*, 52–64, .

23. Giuseppe Mastronuzzi; Paolo Sansò; Large boulder accumulations by extreme waves along the Adriatic coast of southern Apulia (Italy). *Quaternary International* **2004**, *120*, 173-184, 10.1016/j.quaint.2004.01.016.

24. Maria Serafina Barbano; Claudia Pirrotta; F. Gerardi; Large boulders along the south-eastern Ionian coast of Sicily: Storm or tsunami deposits?. *Marine Geology* **2010**, *275*, 140-154, 10.1016/j.margeo.2010.05.005.

25. Nick Marriner; David Kaniewski; Christophe Morhange; Clément Flaux; Matthieu Giaime; Matteo Vacchi; James Goff; Tsunamis in the geological record: Making waves with a cautionary tale from the Mediterranean. *Science Advances* **2017**, *3*, e1700485, 10.1126/sciadv.1700485.

26. Andreas Vott; Hendrik J. Bruins; Matthijs Gawehn; Beverly N. Goodman-Tchernov; P. M. De Martini; Dieter H. Kelletat; Giuseppe Mastronuzzi; Klaus Reicherter; Björn R. Röbke; Anja Scheffers; et al. Publicity waves based on manipulated geoscientific data suggesting climatic trigger for majority of tsunami findings in the Mediterranean – Response to 'Tsunamis in the geological record: Making waves with a cautionary tale from the Mediterranean' by Marriner et al. (2017). *Zeitschrift für Geomorphologie, Supplementary Issues* **2019**, *62*, 7-45, 10.1127/zfg_suppl/2018/0547.

27. Mastronuzzi, G.; Pignatelli, C.; Sansò, P; Boulder fields: A valuable morphological indicator of palaeotsunami in the Mediterranean sea. *Z. Geomorphol. NF* **2006**, *146*, 173–194, .

28. Nott, J; Tsunami or Storm Waves? Determining the Origin of a Spectacular Field of Wave Emplaced Boulders Using Numerical Storm Surge and Wave Models and Hydrodynamic Transport Equations. *J. Coast. Res.* **2003**, *19*, 348–356, .

29. Jonathan Nott; Waves, coastal boulder deposits and the importance of the pre-transport setting. *Earth and Planetary Science Letters* **2003**, *210*, 269-276, 10.1016/s0012-821x(03)00104-3.

30. C. Pignatelli; P. Sansò; G. Mastronuzzi; Evaluation of tsunami flooding using geomorphologic evidence. *Marine Geology* **2009**, *260*, 6-18, 10.1016/j.margeo.2009.01.002.

31. N.A.K. Nandasena; R. Paris; Norio Tanaka; Numerical assessment of boulder transport by the 2004 Indian ocean tsunami in Lhok Nga, West Banda Aceh (Sumatra, Indonesia). *Computers & Geosciences* **2011**, *37*, 1391-1399, 10.1016/j.cageo.2011.02.001.

32. N.A.K. Nandasena; R. Paris; Norio Tanaka; Reassessment of hydrodynamic equations: Minimum flow velocity to initiate boulder transport by high energy events (storms, tsunamis). *Marine Geology* **2011**, *281*, 70-84, 10.1016/j.margeo.2011.02.005.

33. Milella, M.; Scardino, G.; Piscitelli, A.; De Giosa, F.; Locuratolo, G.; Barracane, G; Experimental determination of the friction coefficient for estimating sea storm induced megaboulders movements. *Alp. Mediterr. Quat.* **2018**, *31*, 27–30, .

34. Rónadh Cox; Fabrice Ardhuin; Frédéric Dias; Ronan Autret; Nicole Beisiegel; Claire S. Earlie; James G. Herterich; Andrew Kennedy; Raphaël Paris; Alison Raby; et al. Systematic Review Shows That Work Done by Storm Waves Can Be Misinterpreted as Tsunami-Related Because Commonly Used Hydrodynamic Equations Are Flawed. *Frontiers in Marine Science* **2020**, *7*, 7, 10.3389/fmars.2020.00004.
35. Mastronuzzi, G.; Pignatelli, C; The boulder berm of Punta Saguerra (Taranto, Italy): A morphological imprint of the Rossano Calabro tsunami of April 24, 1836. *Earthplanets Space* **2012**, *64*, 829–842, .
36. Max Engel; Simon Matthias May; Bonaire's boulder fields revisited: evidence for Holocene tsunami impact on the Leeward Antilles. *Quaternary Science Reviews* **2012**, *54*, 126-141, 10.1016/j.quascirev.2011.12.011.
37. Alessio Rovere; Elisa Casella; Daniel L. Harris; Thomas Lorscheid; Napayalage A. K. Nandasena; Blake Dyer; Michael R. Sandstrom; Paolo Stocchi; William J. D'Andrea; Maureen E. Raymo; et al. Giant boulders and Last Interglacial storm intensity in the North Atlantic. *Proceedings of the National Academy of Sciences* **2017**, *114*, 12144-12149, 10.1073/pnas.1712433114.
38. M. Grasso; F. Lentini; Sedimentary and tectonic evolution of the eastern Hyblean Plateau (southeastern Sicily) during late Cretaceous to Quaternary time. *Palaeogeography, Palaeoclimatology, Palaeoecology* **1982**, *39*, 261-280, 10.1016/0031-0182(82)90025-6.
39. F. Cultrera; Giovanni Barreca; Luciano Scarfì; Carmelo Monaco; Fault reactivation by stress pattern reorganization in the Hyblean foreland domain of SE Sicily (Italy) and seismotectonic implications. *Tectonophysics* **2015**, *661*, 215-228, 10.1016/j.tecto.2015.08.043.
40. Bianca, M.; Monaco, C.; Tortorici, L.; Cernobori, L; Quaternary normal faulting in southeastern Sicily (Italy): A seismic source for the 1693 large earthquake. *Geophys. J. Int.* **1999**, *139*, 370–394, .
41. E. Patacca (2) P. Scandone (2); E. Patacca P. Scandone; S. Rossi (7); Mesozoic and Cenozoic Rocks from Malta Escarpment (Central Mediterranean). *AAPG Bulletin* **1981**, *65*, 1299–1319, 10.1306/03b5949f-16d1-11d7-8645000102c1865d.
42. Makris, J.; Nicolich, R.; Weigel, W; A seismic study in the Western Ionian Sea. *Ann. Geophys.* **1986**, *4*, 665–678, .
43. R. Catalano; Carlo Doglioni; S. Merlini; On the Mesozoic Ionian Basin. *Geophysical Journal International* **2001**, *144*, 49-64, 10.1046/j.0956-540X.2000.01287.x.
44. Baratta, M. I Terremoti d'Italia: Saggio di Storia, Geografia e Bibliografia Sismica Italiana; Fratelli Bocca: Torino, Italy, 1901; p. 984.
45. Postpischl, D.C. Catalogo dei Terremoti Italiani Dall'Anno 1000 al 1980; Postpischl, D., Ed.; Consiglio Nazionale Delle Ricerche, Progetto Finalizzato Geodinamica, Sottoprogetto Rischio Sismico e Ingegneria Sismica: Bologna, Italy, 1985; p. 239.
46. Boschi, E.; Guidoboni, E.; Ferrari, G.; Valensise, G.; Gasperini, P. Catalogo dei forti terremoti in Italia dal 461 a.C. al 1990; ING-SGA: Bologna, Italy, 1997; p. 644.
47. Stefano Tinti; Alessandra Maramai; Laura Graziani; The New Catalogue of Italian Tsunamis. *Natural Hazards* **2004**, *33*, 439-465, 10.1023/b:nhaz.0000048469.51059.65.
48. Giovanni Scicchitano; B. Costa; A. Di Stefano; S.G. Longhitano; C. Monaco; Tsunami and storm deposits preserved within a ria-type rocky coastal setting (Siracusa, SE Sicily). *Zeitschrift für Geomorphologie, Supplementary Issues* **2010**, *54*, 51-77, 10.1127/0372-8854/2010/0054s3-0019.